Accepted Manuscript

Energy and exergy analyses of sewage sludge thermochemical treatment

María Atienza-Martínez, Javier Ábrego, José Francisco Mastral, Jesús Ceamanos, Gloria Gea

PII: S0360-5442(17)32026-1

DOI: 10.1016/j.energy.2017.12.007

Reference: EGY 11956

To appear in: *Energy*

Received Date: 30 October 2017

Revised Date: 1 December 2017

Accepted Date: 3 December 2017

Please cite this article as: Atienza-Martínez Marí, Ábrego J, Mastral JoséFrancisco, Ceamanos Jesú, Gea G, Energy and exergy analyses of sewage sludge thermochemical treatment, *Energy* (2018), doi: 10.1016/j.energy.2017.12.007.

Energy and exergy analyses of sewage sludge thermochemical treatment

María Atienza-Martínez[a]*, Javier Ábrego[a], José Francisco Mastral[a], Jesús Ceamanos[a], Gloria Gea[a]

[a]Thermochemical Processes Group (GPT), Aragón Institute for Engineering Research (I3A), Universidad de Zaragoza, Edificio I+D, C/ Mariano Esquillor s/n, 50018 Zaragoza, Spain

*Corresponding Author

Telephone: +34876555483 Fax: +34976761879

e-mail: atienza@unizar.es

ABSTRACT

The aim of this research was to provide a methodology for calculating the energy and exergy balances for the thermochemical treatment of sewage sludge. The results of the balances were assessed and compared for three different scenarios (torrefaction, pyrolysis and pyrolysis combined with catalytic post-treatment of the vapors). The balances were calculated based on previously published experimental data and evaluated under different conditions. The results indicated that the endothermicity decreased with the severity of the process. The energy recovery from the products favored the exothermicity of the processes. The three-step process (pyrolysis of torrefied sewage sludge combined with catalytic post-treatment of the hot vapors) was the least exergy efficient scenario.

Keywords: Torrefaction; Pyrolysis; Catalytic post-treatment; Sewage sludge; Energy balance; Exergy balance.

Nomenclature:

AP: aqueous phase.

C_p: specific heat capacity at constant pressure, $MJ \cdot kg^{-1} \cdot K^{-1}$.

e: specific exergy, $MJ \cdot kg^{-1}$.

h: specific enthalpy, $MJ \cdot kg^{-1}$.

h_{vap}: specific enthalpy of evaporation $MJ \cdot kg^{-1}$.

HOP: heavy organic phase.

LOP: light organic phase.

NCG. non-condensable gases.

OP: organic phase.

P: pressure, Pa.

P_0: pressure at the standard reference state, $1.01 \cdot 10^5$ Pa.

Q: enthalpy required, $MJ \cdot kg^{-1}$.

R: universal gas constant, 8.314472 kJ $kmol^{-1}$ K^{-1}.

s: specific entropy, $MJ \cdot kg^{-1}$.

T: temperature, K.

T_b: boiling temperature, K.

T_p: process temperature, K.

T_0: temperature at the standard reference state, 298.15 K.

SS: sewage sludge.

TSS: torrefied sewage sludge.

x: mass fraction, expressed as a decimal.

W: water content, mass fraction %.

z: height.

Abbreviations:

HHV: higher heating value, $MJ \cdot kg^{-1}$.

LHV: lower heating value, $MJ \cdot kg^{-1}$ or $MJ \cdot m^{-3}$ (STP).

Superscripts:

0: at 25 °C and $1.01 \cdot 10^5$ Pa.

Subscripts:

b: boiling.

cat: with catalytic treatment of pyrolysis vapors.

ch: chemical.

ph: physical.

db: dry basis.

i, j: i, j-th species.

input: incoming stream.

f: formation.

feedstock: material fed to the process.

gas: in gaseous state.

liquid: in liquid form.

liquid,phase: phase present in the liquid.

NCG. non-condensable gases.

oc: representative organic compound.

output: exiting stream.

p: process.

ph: physical.

process: process.

pyr: pyrolysis.

solid: solid compound.

SS: sewage sludge.

TSS: torrefied sewage sludge.

torr: torrefaction.

water: water.

0: at 298.15 K and $1.01 \cdot 10^5$ Pa.

Greek letters:

β: ratio of standard specific chemical exergy to the lower heating value.

Δh: enthalpy difference at a given temperature, $MJ \cdot kg^{-1}$.

λ: latent heat of vaporization of water, $MJ \cdot kg^{-1}$.

η: yield of product, mass fraction %.

Ψ: overall exergy efficiency, %.

1. Introduction

Biomass and biomass waste are considered promising renewable energy sources, since the reserves of fossil fuels are running out and in any case their use is responsible for global warming. Thermochemical treatment is one of the options for exploiting biomass for energy purposes. Among thermochemical processes, pyrolysis can yield a major bio-oil fraction which has potential use as a fuel or as a source of chemical products. The energy analysis of the pyrolysis process is useful for comparing the energy

requirements with those of other alternatives for fuel production. Overall, the pyrolysis and torrefaction processes are regarded as endothermic; consequently, their energy analyses are also of great interest for the scaling of the installations from lab-scale to commercial scale [1].

Reed and Cowdery [2] differentiated between heat of pyrolysis and heat for pyrolysis. These authors defined heat of pyrolysis as the heat needed to decompose biomass into different products (char, liquid and non-condensable gases) at the pyrolysis temperature, and heat for pyrolysis as the sum of the heat of pyrolysis and the sensible heat needed to raise biomass to the pyrolysis temperature. Pyrolysis has been considered globally endothermic, although both exothermic and endothermic values of heat of pyrolysis have been reported in the literature, since this process comprises exothermic and endothermic steps [3]. For example, Mok and Antal [4] stated that formation of char and gas in secondary reactions are exothermic, while tar formation and evaporation are endothermic. Chen et al. [5] observed changes in the thermal behavior of biomass (from endothermic to exothermic) as the conversion ratio increased. According to several authors [1, 6-8], the enthalpy for torrefaction or pyrolysis of a particular feedstock comprises both the energy required to heat the material and to decompose it into the different products, coinciding with the definition of heat for pyrolysis provided by Reed and Cowdery [2]. Thus, it includes the sensible energy (absorbed by biomass to increase its temperature) and the energy of reaction (necessary for torrefaction or pyrolysis reactions). This last approach requires the determination of the heat requirement of the pyrolysis reaction by techniques such as differential scanning calorimetry (DSC). Several authors have analyzed qualitatively and quantitatively by DSC the heat required for pyrolysis of lignocellulosic biomass and wastes [3-5, 9-11]. Generally, the heat for pyrolysis reactions is much lower than the sensible and the latent heats and can be considered negligible.

There are different ways to address the energy balances. Boateng et al. [12] evaluated the energy analysis of the production of bio-oil by fast pyrolysis in terms of calorific values. Recently, Hasokai et al. [13] suggested an alternative approach, which involves the estimation of heating values based on the elemental composition of solid and liquid fractions. Capodaglio et al. [14] carried out a preliminary energy balance of microwave-induced pyrolysis of sewage sludge based on the power irradiated by the mono-modal microwave synthesizer used as a source of energy. Boukis et al. [8] determined the heat of pyrolysis by using empirical correlations based on the moisture and ash contents of the biomass. Although pyrolysis products are complex in nature and their standard enthalpies of formation and specific heat capacities are not always easy to determine [1], the energy balance can also be evaluated in terms of the difference

between the enthalpy of reactants and products [3, 15, 16]. This is the methodology applied in the present work.

Energy analyses provide the quantity of energy required by a certain process but not its quality. Exergy is a thermodynamic property that gives an idea of the quality of energy. It can be defined as the theoretical maximum amount of useful work that can be obtained from the interaction between a certain thermodynamic and its surroundings. Exergy analysis is based on both the first and the second laws of thermodynamics, and allows the determination of the maximum useful work of a process [17]. The presence of exergy losses means that the thermodynamics of the process can be potentially improved. Thus, the exergy analyses help to identify the process improvements needed and to compare alternatives. Exergy analysis has been used for improving life cycle analysis of renewable energy [18, 19].

The exergy analysis of material streams crossing system boundaries comprises kinetic, potential, physical and chemical terms. Kinetic exergy is related to the velocity of a stream with respect to a fixed reference frame. Potential exergy is related to the position of a body in a given force field. Physical exergy is the maximum work obtainable when bringing a substance from its initial state to the thermodynamic environment by physical processes [17]. Chemical exergy is the maximum amount of work that can be obtained when a substance or a mixture is brought from the reference-environment state to the dead state by heat transfer and exchange of substances with the reference environment [17, 20]. Kinetic and potential exergies are usually neglected in pyrolysis processes owing to their small values. Due to the complex nature of carbon based pyrolysis feedstocks (including wastes and lignocellulosic biomass) and products, it is complicated to calculate their chemical exergy. Various models and correlations have been developed to estimate the chemical exergy of such substances [21-27].

The energy analysis of the thermochemical treatment of sewage sludge (SS) by means of torrefaction and pyrolysis has barely been investigated, apart from the energetic assessments carried out by Ding and Jiang [28], Caballero et al. [29], Kim and Parker [30], Ábrego et al. [31], Gil-Lalaguna et al. [32], Capodaglio et al. [14] and Ruiz-Gómez et al. [33]. Exergy analyses of processes such as torrefaction and pyrolysis of biomass are not very common in the literature [12, 34-38] and the information about the exergy analysis of the thermochemical treatment of sewage sludge is even scarcer. Given this little information available and its usefulness when evaluating the feasibility of these processes, the aim of the present work was to assess the energy and exergy analyses of sewage sludge utilization by different thermochemical treatments (specifically, torrefaction and pyrolysis). These analyses were based on experimental data,

which in turn allowed the evaluation of the differences in the heat required for the different processes and the exergy efficiency. The methodology for determining both energy and exergy analyses of thermochemical treatment of biomass in general is provided.

2. Methodology

This section includes the different scenarios studied, the assumptions and simplifications made, and the methodology followed for the energy and exergy balances calculations.

2.1. Scenarios

The different scenarios considered in the present work for the thermochemical treatment of SS are described below.

2.1.1. Torrefaction

Torrefaction has been considered as a pretreatment for the further thermochemical treatment of biomass, including SS [31, 39, 40]. The experimental data used in the present paper can be found elsewhere [41]. Torrefaction was performed in an auger reactor at temperatures between 250-300 °C and solid residence times between 13-35 min. The products obtained were torrefied sewage sludge (TSS), non-condensable gases (NCG_{torr}) and a liquid product that separated into an organic phase (OP_{torr}) and an aqueous phase (AP_{torr}). A block diagram of the torrefaction process (with input and output streams, and the products either at the standard reference state or at the process conditions) is shown in Figure 1.

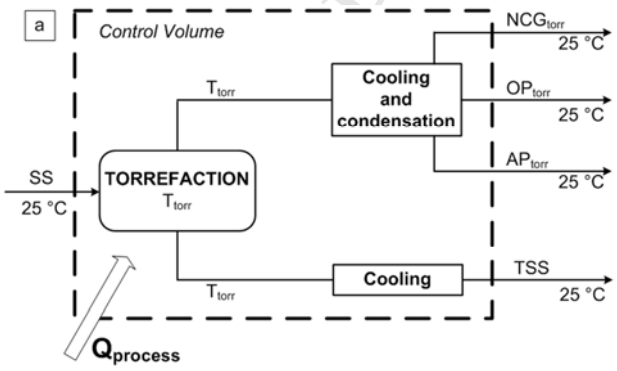

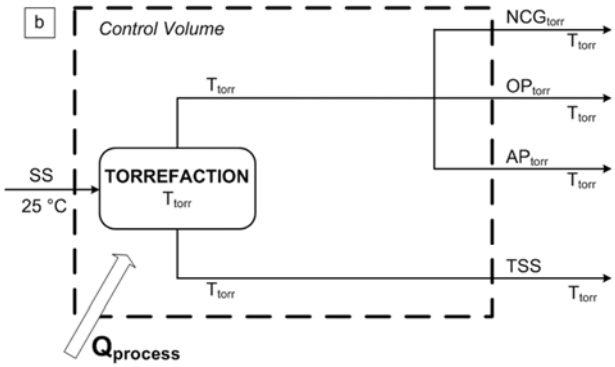

Figure 1. Control volume for torrefaction. (a) Products at the standard reference state. (b) Products at process conditions.

2.1.2. Pyrolysis

Pyrolysis of SS for the production of liquid fuels has been previously studied [42]. Pyrolysis of TSS has also been investigated in order to improve the properties of the liquid product for use as a fuel. The experimental data used in the present paper for the energy and exergy analyses of pyrolysis of both SS and TSS (see block diagrams in Figure 2) can be found elsewhere [39]. Pyrolysis was carried out in a fluidized bed reactor at 530 °C with a solid residence time of 5.7 min. The energy and exergy balances were analyzed in the case of pyrolysis of SS and TSS obtained in an auger reactor at 250 °C and 13 min (TSS250), and at 275 °C and 24 min (TSS275). The choice of these torrefaction conditions was based on the compromise reached between a low yield of organic compounds and a high yield of water during torrefaction. The products obtained were char ($Char_{pyr}$), non-condensable gases (NCG_{pyr}) and a liquid product that separated into a light organic phase (LOP_{pyr}), a heavy organic phase (HOP_{pyr}) and an aqueous phase (AP_{pyr}). The results of the analyses provided information about how the changes underwent by the solid during the torrefaction step affected the pyrolysis step.

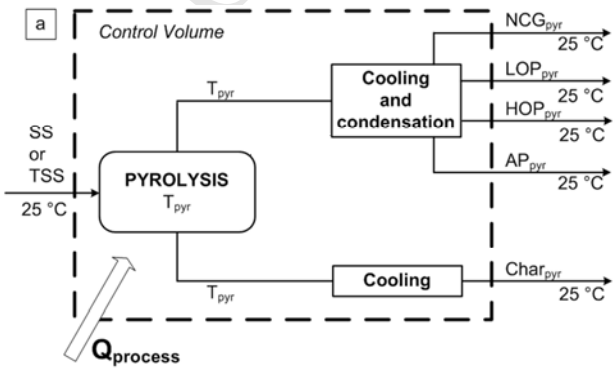

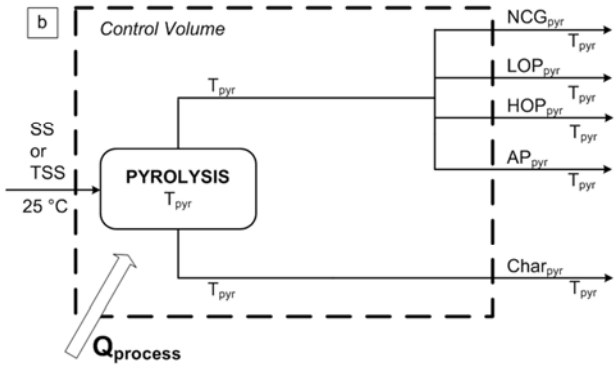

Figure 2. Control volume for pyrolysis. (a) Products at the standard reference state. (b) Products at process conditions.

In the case of TSS, the balances can also be analyzed considering a combined process of torrefaction and pyrolysis (block diagrams shown in Figure 3). These analyses provided information about how torrefaction affected the overall process.

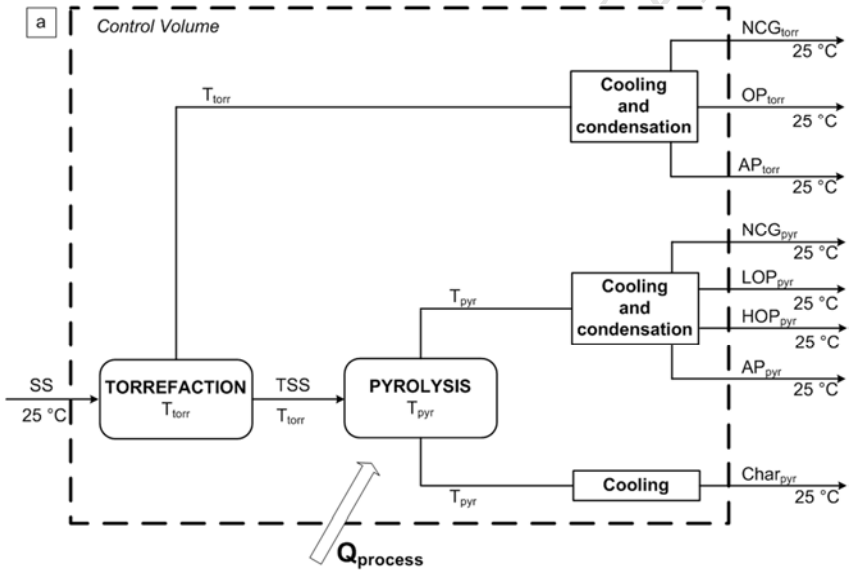

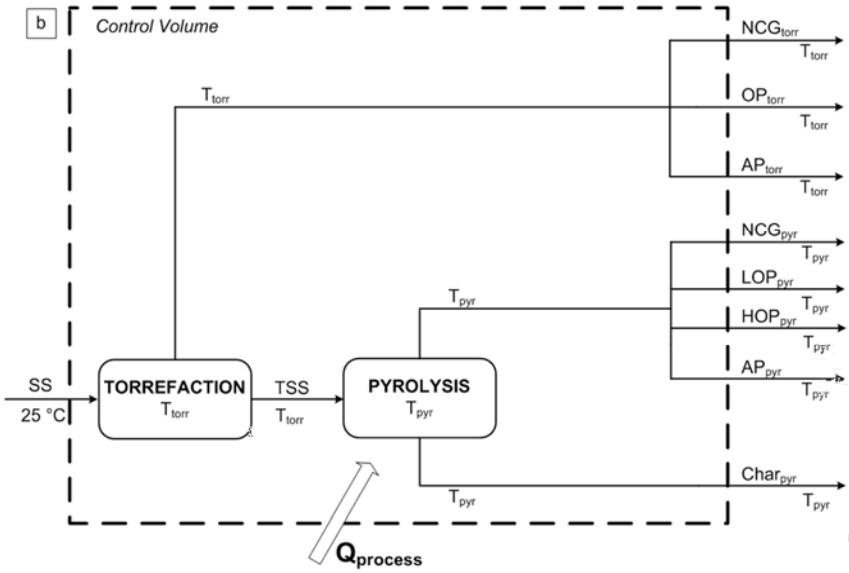

Figure 3. Control volume for pyrolysis including the torrefaction step. (a) Products at the standard reference state. (b) Products at process conditions.

2.1.3. Pyrolysis with catalytic post-treatment of the hot pyrolysis vapors

The energy and exergy balances of pyrolysis of both SS and TSS with catalytic post-treatment of the hot vapors were evaluated. The main goal of combining torrefaction pre-treatment with catalytic post-treatment of the hot pyrolysis vapors was to enhance the fuel properties of the pyrolysis liquid. The experimental procedure and results were shown elsewhere [43]. Pyrolysis was carried out in a fluidized bed reactor at 530 °C with a solid residence time of 5.7 min. A lab-scale fixed bed reactor connected downstream to the fluidized bed reactor was used to carry out the catalytic post-treatment of the hot pyrolysis vapors at 480 °C using γ-Al_2O_3. The energy and exergy balances were analyzed in the case of pyrolysis of SS and SS torrefied in an auger reactor at 250 °C and 13 min, and at 275 °C and 24 min. The products obtained were char ($Char_{cat}$), non-condensable gases (NCG_{cat}) and a liquid product that separated into an organic phase (OP_{cat}) and an aqueous phase (AP_{cat}). The analyses provided information about both how the changes suffered by the solid during torrefaction affected the subsequent treatments and how the catalytic post-treatment of the hot pyrolysis vapors affected the heat requirements and exergy efficiency (see block diagrams in Figure 4).

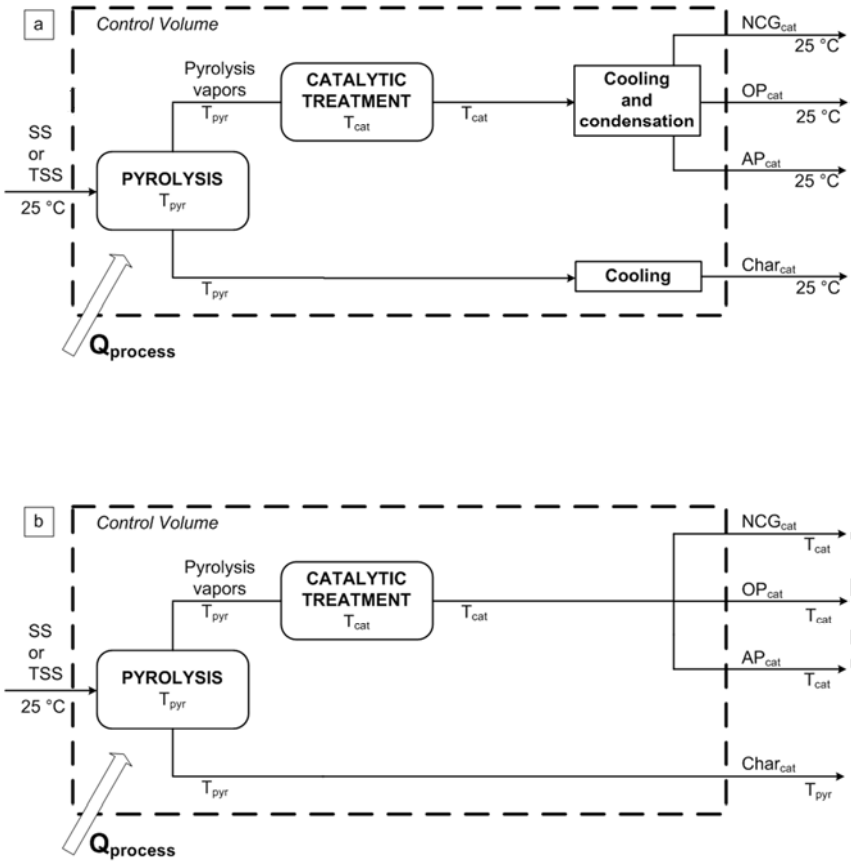

Figure 4. Control volume for pyrolysis with catalytic treatment of the vapors. (a) Products at the standard reference state. (b) Products at process conditions.

In the case of TSS, the balances can also be analyzed considering the three steps (torrefaction, pyrolysis and catalytic post-treatment of the hot vapors) globally (block diagrams shown in Figure 5). These analyses provided information about how torrefaction affected the whole process.

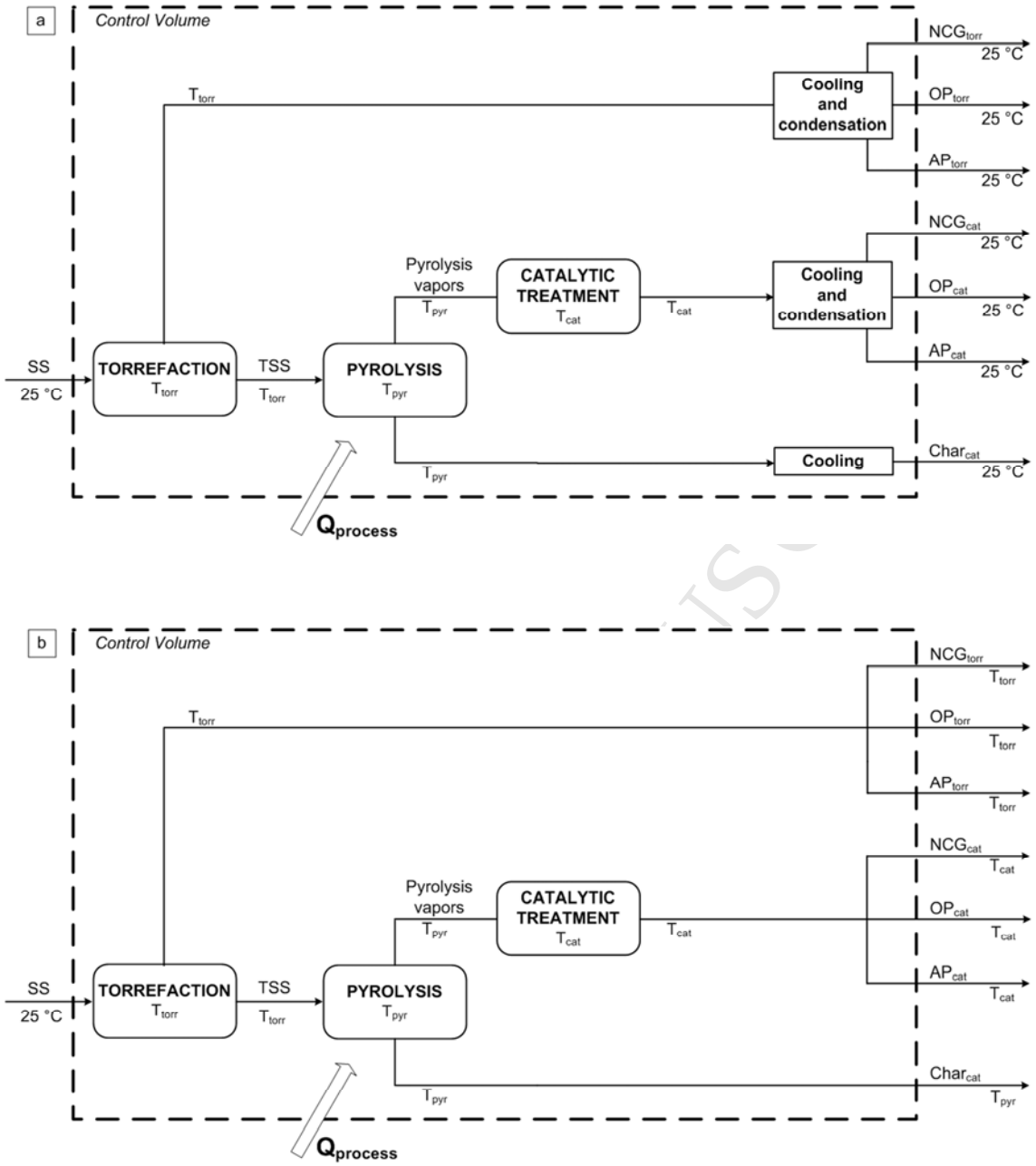

Figure 5. Control volume for pyrolysis with catalytic post-treatment of the hot vapors, including the torrefaction step. (a) Products at the standard reference state. (b) Products at process conditions.

2.2. Assumptions

The following assumptions, simplifications and stream properties were adopted for the energy and exergy balances:

- The standard reference state was T_0 = 25 °C and $P_0 = 1.01 \cdot 10^5$ Pa.
- The characterization of the different streams is shown in Appendix A.

- SS was thermally dried prior to any thermochemical treatment and the heat needed for that step should be considered for the energy balances. The energy requirements for the thermal drying was previously estimated [3]. Almost 8 MJ per kg of 6.5% dried SS were required to reduce the moisture content of dewatered SS from 77% to 6.5%.
- The energy and exergy balances of the different processes studied were assessed in two ways. On the one hand, it was assumed that both the sensible and latent heat of all the products obtained was efficiently recovered. On the other hand, it was considered that no energy from the products was recovered, that is, the temperature of the products was the process temperature.
- The experimental data used for the calculations were obtained in different lab-scale installations (fluidized bed reactor and auger reactor ~ 1-2 $kg \cdot h^{-1}$) which have been shown elsewhere [39, 41, 43] (they can also be found in Appendix A).
- The specific heat capacity of TSS was considered the same regardless of the torrefaction conditions and constant with temperature, using an experimental value obtained at 25 °C ($1.21 \cdot 10^{-3}$ $MJ \cdot kg^{-1} \cdot K^{-1}$). The specific heat capacity of char was considered constant with temperature using an average experimental value ($0.95 \cdot 10^{-3}$ $MJ \cdot kg^{-1} \cdot K^{-1}$) experimentally obtained at between 25 °C and 300 °C.
- Liquid phases were considered to be ideal solutions.
- When needed, it was assumed that the liquid phases consisted of water and an organic compound selected as representative compound of the organic fraction of the phase.
- The major organic compound in each liquid phase in terms of chromatographic area was chosen as representative. These are listed in Table 1.

Table 1. Representative organic compounds chosen for the liquid phases.

Process	Phase	Representative organic compound
Torrefaction	AP_{torr}	Acetic acid
	OP_{torr}	Hexadecanoic acid
Pyrolysis	AP_{pyr}	Acetic acid
	HOP_{pyr}	3-Methylphenol
	LOP_{pyr}	Cholest-4-ene
Pyrolysis with catalytic post-treatment	AP_{cat}	Acetonitrile
	OP_{cat}	3-Methylphenol

- The specific heat capacity of water and the representative organic compounds in liquid form was considered constant with temperature.
- Thermodynamic properties of liquid and gaseous compounds were obtained from the literature [44, 45].
- Experiments performed in the fluidized bed reactor required the introduction of a large flow of N_2. Heating this N_2 flow up to the process temperature could impact the heat requirements. Experiments performed in the auger reactor required lower N_2 flows; consequently, the heating of the N_2 flow has a lower impact on the heat requirements. The heat necessary to heat the N_2 flow was not taken into account.
- Heat losses were not taken into account in this study. In industrial practice, heat loss estimation may be relevant, and values may largely differ depending on the reactor system. Several works have estimated heat losses as a percentage of $Q_{process}$ obtaining values that vary from 1 % [1] to 9 % [7].
- The estimation of $Q_{process}$ with energy recovery provided a maximum reference value for the energy efficiency of the thermochemical processes considered.
- It was assumed that the terms regarding the kinetic and potential exergy were negligible [46].
- For the exergy analyses, all the products were considered useful. None of them was considered as a waste or as needed for use within the process itself.
- An active Excel spreadsheet for energy and exergy balance calculation is provided as Supplementary Material.

Some remarks must be done regarding the energy analyses, especially of the processes represented in Figures 1b-5b, with products exiting the system at the process temperature. In these cases, relatively large deviations of $Q_{process}$ can be obtained as a result of several uncertainties, such as the incomplete knowledge of liquid compositions and thermodynamic properties of the relevant compounds. Taking the liquid phase compositions as formed only by representative compounds from Table 1 is a clear oversimplification; nevertheless, other alternative approaches (such as making a weighted average of several detected compounds) are hindered by (i) the lack of available thermodynamic data for such species, and (ii) the semi-quantitative nature of the analytical technique used for determining liquid compositions. Therefore, values from these analyses are provided mainly for comparison between the different thermochemical treatments presented in this work, and care must be taken when comparing the

obtained values to other obtained with different feedstock and operational conditions. In the case of $Q_{process}$ determined with products exiting at 25 ºC, results are much less affected by the mentioned uncertainties (that only apply to a small fraction of the aqueous phase).

2.3. Energy assessment

The procedure followed for the energy balance calculations was similar to those used by Ábrego et al. and Gil-Lalaguna et al. [31, 32]. Unlike the present work, Ábrego et al. [31] only determined the heat required for the process in the case that both feedstock and products were considered to be at the standard reference state. Gil-Lalaguna et al. [32] calculated the energy balance for pyrolysis considering the products at the process conditions. However, they only considered one set of pyrolysis conditions and did not study the effect of the process conditions or the combination of processes on the heat required. Furthermore, exergy balances were not performed in either of the two studies.

A detailed explanation of the procedure followed in this study is presented below. The energy process requirement that should be supplied externally ($Q_{process}$) was calculated as the difference between the enthalpy output (h_{output}) and input (h_{input}). Thus, the enthalpy balances were expressed by Equation 1.

$$Q_{process} + h_{input} = h_{output} \quad \text{Equation 1}$$

where:

$Q_{process}$: enthalpy process requirement that should be supplied externally, $MJ \cdot kg^{-1}$.

h_{input}: specific input enthalpy, $MJ \cdot kg^{-1}$.

h_{output}: specific output enthalpy, $MJ \cdot kg^{-1}$.

2.3.1. Enthalpy calculation

The only energy input considered was the energy of the feedstock (SS or TSS). Energy outputs were those of the different products obtained: solid, liquid and NCG. The enthalpy of the input stream (h_{input}) was always calculated using Equation 2.

$$h_{input} = \Delta h^{0}_{f,feedstock} \quad \text{Equation 2}$$

where:

$\Delta h^{0}_{f,feedstock}$: standard enthalpy of formation estimated for the feedstock, $MJ \cdot kg^{-1}_{feedstock}$.

The enthalpy of the output stream (h_{output}) was calculated using Equation 3.

$$h_{output} = h_{NCG} + h_{solid} + \sum_i h_{liquid\ phase,i}$$ Equation 3

where the subscripts refer to NCG, solid and liquid phase i exiting the reactor.

When the feedstock and the products were considered to be at the standard reference state (assuming that both the sensible and the latent heat of all the products obtained was efficiently recovered) the h_{output} was calculated using Equation 4.

$$h_{output} = \frac{\left(\sum_i \eta_i \cdot \Delta h^0_{f,i}\right)}{100}$$ Equation 4

where:

η_i: yield of product i, mass fraction %.

$\Delta h^0_{f,i}$: standard enthalpy of formation estimated for product i, $MJ \cdot kg^{-1}_{product,\ i}$.

When the products leave the system at the process conditions, h_{NCG}, h_{solid} and h_{liquid} were calculated as follows.

The h_{NCG} was calculated by Equation 5:

$$h_{NCG} = \frac{\eta_{NCG} \cdot \left(\Delta h^0_{f,NCG} + \left(\sum_i x_i \cdot \int_{T_0}^{T_p} Cp_{gas,i}(T) \cdot dT\right)\right)}{100}$$ Equation 5

where:

η_{NCG}: yield of NCG, mass fraction %.

x_i: mass fraction of component i in the NCG, expressed as a decimal.

The h_{solid} was calculated by Equation 6:

$$h_{solid} = \frac{\eta_{solid} \cdot (\Delta h^0_{f,solid} + Cp_{solid} \cdot (T_p - T_0))}{100}$$ Equation 6

where:

η_{solid}: yield of solid product, mass fraction %.

The calculation of the enthalpy of the liquid product (h_{liquid}) took into account the presence of the different liquid phases (Equation 7).

$$h_{liquid}=\frac{\left(\sum_i \eta_{liquid\ phase,i}\cdot h_{liquid\ phase,i}\right)}{100}$$ Equation 7

where:

$\eta_{liquid\ phase,i}$: yield of phase i, mass fraction %.

$h_{liquid\ phase,i}$ was calculated by Equation 8.

$$h_{liquid\ phase,i}=\frac{\eta_{liquid\ phase,i}}{100}\cdot\left(\frac{W_{liquid\ phase,\ i}\cdot h_{water}+\left(100-W_{liquid\ phase,\ i}\right)\cdot h_{oc,i}}{100}\right)$$ Equation 8

where:

$W_{liquid\ phase,i}$: water content of phase i, mass fraction %.

$h_{oc,i}$ was calculated by Equation 9, while h_{water} was obtained from the literature [45].

$$h_{oc,i}=(\Delta h^0_{f,oc,i}+\Delta h_{vap,oc,i}+Cp_{oc,i,liquid}\cdot(T_{b,oc,i}-T_0)+\int_{T_{b,oc,i}}^{T_p} Cp_{oc,i,gas}\,(T)\cdot dT))$$ Equation 9

2.3.1.1. Standard enthalpy of formation

The standard enthalpy of formation (Δh_f^0) of the NCG was calculated as the weighted average of the Δh_f^0 of each one of the components of this stream. The composition of the NCG streams was experimentally determined by gas chromatography. The Δh_f^0 data of the gases forming the NCG stream can be found in the literature [44].

The Δh_f^0 estimated for the solid and the liquid organic phases was calculated by applying the Hess law, following Equation 10 [47], using their ultimate analyses and higher heating values (HHV), which were experimentally measured. The Δh_f^0 data of the gases obtained from the complete combustion of the solids and the organic phases can be found in the literature [44].

$$\Delta h^0_{f,i}=\left(\sum_j x_j\cdot\Delta h^0_{f,j}\right)+HHV_i$$ Equation 10

where:

x_j: mass fraction of the product j obtained from the complete combustion of material i, expressed as per unit.

$\Delta h^0_{f,j}$: standard enthalpy of formation of the product j obtained from the complete combustion of material i, $MJ\cdot kg^{-1}_{product,j}$.

HHV_i: higher heating value of material i, $MJ \cdot kg^{-1}_{material,i}$.

It was not possible to measure the HHV of the AP due to the high water content. Then, the $\Delta h^0_{f,AP}$ was calculated as the weighted average of the Δh^0_f of water ($\Delta h^0_{f,water}$) and the Δh^0_f of the representative organic compound ($\Delta h^0_{f,oc,i.}$), by using Equation 11.

$$\Delta h^0_{f,AP} = \frac{W_{AP}}{100} \cdot \Delta h^0_{f,water} + \frac{(100-W_{AP})}{100} \cdot \Delta h^0_{f,oc,i.} \quad \text{Equation 11}$$

where:

$\Delta h^0_{f,AP}$: enthalpy of formation of the aqueous phase, $MJ \cdot kg^{-1}_{AP}$.

W_{AP}: water content of the aqueous phase, mass fraction %.

2.3.1.2. Specific heat capacity

As mentioned above, the composition of the liquid phases was simplified considering only water and the representative organic compound. The mass of the representative organic compound in each phase was equated to the whole organic fraction in the phase. The specific heat capacity data of the representative organic compounds (liquid or vapor) and water (liquid or steam) can be found in the literature [45].

The specific heat capacity of each NCG component can be calculated by the correlation given in Equation 12 [48].

$$Cp_{gas,i} = \int_{T_0}^{T} \left(a + b \cdot T + c \cdot T^2 + d \cdot T^3\right) dT \quad \text{Equation 12}$$

where:

a, b, c, d: coefficients of constant pressure specific heat capacity, $MJ \cdot kg^{-1}$.

2.4. Exergy assessment

The exergy balance for a certain system can be expressed by Equation 13. The exergy losses are comprised of the heat released to the surroundings by the by-products and the irreversibilities [17]. These irreversibilities within the system cause exergy destruction and thus exergy does not obey the conservation law.

$$\sum e_{input} = \sum e_{output} + \sum e_{loss} \quad \text{Equation 13}$$

where:

$\sum e_{input}$: exergy content of the input streams, $MJ \cdot kg_{SS}^{-1}$.

$\sum e_{output}$: exergy content of the output streams, $MJ \cdot kg_{SS}^{-1}$.

$\sum e_{loss}$: exergy losses, $MJ \cdot kg_{SS}^{-1}$.

Taking into account that the terms regarding the kinetic and potential exergy were considered negligible [46], the exergy of a certain stream is comprised of the chemical and the physical exergies (Equation 14).

$$e=e_{ch}+e_{ph} \quad \text{Equation 14}$$

where:

e_{ch}: chemical exergy, $MJ \cdot kg^{-1}$.

e_{ph}: physical exergy, $MJ \cdot kg^{-1}$.

The exergy associated to the heat required for the process is given by Equation 15:

$$e_Q=Q_{process} \cdot \left(1-\frac{T_0}{T_p}\right) \quad \text{Equation 15}$$

where:

e_Q: thermal exergy, $MJ \cdot kg^{-1}$.

The overall exergy efficiency (Ψ) of each process was calculated in terms of exergy using Equation 16, taking into account the exergy associated to the heat required for the process in the input stream.

$$\psi=100 \cdot \frac{\Sigma e_{output}}{\Sigma e_{input}} \quad \text{Equation 16}$$

2.4.1. Chemical exergy calculation

When both the starting material and the different products obtained were considered to be at the standard reference state of temperature and pressure, the exergy was equal to the chemical exergy, which is that of a certain compound at the standard reference state. The chemical exergy of several compounds can be

found in the literature. However, it was not easy to define the chemical exergy of SS and the solid and liquid products from torrefaction and pyrolysis, since they consist of many substances. There are different correlations to estimate the chemical exergy of solid and liquid fuels. The chemical exergy can be calculated as the product of the lower heating value (LHV) and an exergy coefficient. The correlation suggested by Szargut et al. [46] has been commonly used to calculate the chemical exergy of biomass. Hepbasli [49] also proposed an equation to determine the chemical exergy of biomass. In the present work, the chemical exergy of SS, TSS and char was estimated using the equations used by Kaushik and Singh for moist solid fuels with non-negligible sulfur and ash contents [50]. These equations (Equation 17 and Equation 18) relate the ultimate analysis and the calorific value of the solids with the chemical exergy.

$$e_{ch.solid}=(LHV_{db}+\lambda\cdot x_m)\cdot\beta_{db}+9417\cdot x_{S,db} \quad \text{Equation 17}$$

where:

$e_{ch,solid}$: specific chemical exergy of solid streams, $MJ\cdot kg_{solid}^{-1}$.

LHV_{db}: lower heating value of the solid on a dry basis, $MJ\cdot kg_{solid}^{-1}$.

λ: latent heat of vaporization of water at 25 °C, $MJ\cdot kg_{water}^{-1}$

x_m: mass fraction of moisture.

β_{db}: ratio of standard specific chemical exergy to the LHV on a dry basis.

$x_{S,db}$: mass fraction of sulfur on a dry basis.

$$\beta_{db}=1.0437+0.1882\cdot\frac{x_{H,db}}{x_{C,db}}+0.0610\cdot\frac{x_{O,db}}{x_{C,db}}+0.0404\cdot\frac{x_{N,db}}{x_{C,db}} \quad \text{Equation 18}$$

where:

$x_{i,db}$: mass fraction of a certain element on a dry basis.

For the calculation of the chemical exergy in the case of the liquid phases, the assumption that these streams consisted of water and a representative organic compound was also made. Thus, the $e_{ch,liquid\ phase,i}$ was calculated using Equation 19.

$$e_{ch,liquid\ phase,i}=\frac{W_{liquid\ phase,i}}{100}\cdot e_{ch,water}+\frac{(100-W_{liquid\ phase,i})}{100}\cdot e_{ch,oc,i} \quad \text{Equation 19}$$

where:

$e_{ch,water}$: chemical exergy of water, $MJ \cdot kg^{-1}_{water}$ [45].

$e_{ch,oc,i.}$: chemical exergy of the representative organic compound in phase i, $MJ \cdot kg^{-1}_{OC,i}$ [45].

For the calculation of the chemical exergy of the NCG ($e_{ch,NCG}$), it was considered that the gaseous streams behaved as ideal gases. Thus, the chemical exergy of the NCG stream can be expressed by Equation 20.

$$e_{ch,NCG} = \sum_i x_{gas,i} \cdot e_{ch,gas,i} + R \cdot T_0 \cdot \sum_i x_{gas,i} \cdot \ln x_{gas,i} \quad \text{Equation 20}$$

where:

$x_{gas,i}$: mass fraction of a certain gas component.

$e_{ch,gas,i}$: specific chemical exergy of a certain gas component, $MJ \cdot kg^{-1}_{gas,i}$ [45].

2.4.2. Physical exergy calculation

When the products from the different processes evaluated were considered to be at the process conditions, both the chemical and the physical exergies were taken into account for the calculation of the exergy balances. The physical exergy is given by Equation 21 (which involves Equation 22 and Equation 23).

$$e_{ph,i} = (h - h_0) - T_0 \cdot (s - s_0) \quad \text{Equation 21}$$

$$h - h_0 = \int_{T_0}^{T} Cp\,dT \quad \text{Equation 22}$$

$$s - s_0 = \int_{T_0}^{T} \frac{Cp}{T}\,dT - R \cdot \ln \frac{P}{P_0} \quad \text{Equation 23}$$

where:

h: specific enthalpy at the process conditions, $MJ \cdot kg^{-1}$.

h_0: specific enthalpy at the standard reference state, $MJ \cdot kg^{-1}$.

s: specific entropy at the process conditions, $MJ \cdot kg^{-1}K^{-1}$.

s_0: specific entropy at the standard reference state, $MJ \cdot kg^{-1}K^{-1}$.

P: process pressure, Pa.

P_0: reference pressure, $1.01 \cdot 10^5$ Pa.

Since the processes were performed at atmospheric pressure, Equation 22 results in Equation 24.

$$e_{ph,i} = \int_{T_0}^{T} Cp\,dT - T_0 \cdot \int_{T_0}^{T} \frac{Cp}{T}\,dT \quad \text{Equation 24}$$

The physical exergy of solids and liquids is usually small compared to their chemical exergy. The physical exergy of the solids ($e_{ph,solid}$) was calculated using Equation 25.

$$e_{ph,solid} = \int_{T_0}^{T} Cp_{solid}\,dT - T_0 \cdot \int_{T_0}^{T} \frac{Cp_{solid}}{T}\,dT \quad \text{Equation 25}$$

where:

$e_{ph,solid}$: physical exergy of solid product, $MJ \cdot kg^{-1}_{solid}$.

Cp_{solid}: specific heat capacity of solid product, $MJ \cdot kg^{-1}_{solid.}$

For the calculation of the physical exergy of the liquid phases, they were considered again as a mixture of water and the selected representative organic compound (Equation 26).

$$e_{ph,liquid\ phase,i} = \frac{W_{liquid\ phase,i}}{100} \cdot e_{ph,water} + \frac{(100 - W_{liquid\ phase,i})}{100} \cdot e_{ph,oc,i} \quad \text{Equation 26}$$

where:

$e_{ph,liquid\ phase,i}$: physical exergy of the liquid phase i, $MJ \cdot kg^{-1}_{liquid\ phase,i}$.

$e_{ph,water}$: physical exergy of water, $MJ \cdot kg^{-1}_{water}$.

$e_{ph,oc,i}$: physical exergy of the representative organic compound of liquid phase i, $MJ \cdot kg^{-1}_{oc,i}$.

$e_{ph,water}$ can be calculated using Equation 27.

$$e_{ph,water} = \int_{T_0}^{T} Cp_{water}\,dT - T_0 \cdot \int_{T_0}^{T} \frac{Cp_{water}}{T}\,dT \quad \text{Equation 27}$$

where:

Cp_{water}: specific heat capacity of water [44], $MJ \cdot kg^{-1}_{water.}$

$e_{ph,oc,i}$ can be calculated using Equation 28.

$$e_{ph,oc,i} = \int_{T_0}^{T} Cp_{oc,i}\,dT - T_0 \cdot \int_{T_0}^{T} \frac{Cp_{oc,i}}{T}\,dT \quad \text{Equation 28}$$

where:

$Cp_{oc,i}$: specific heat capacity of the representative organic compound of liquid phase i [44], $MJ \cdot kg^{-1}_{oc,i.}$

For the calculation of the physical exergy of the NCG streams ($e_{ph,NCG}$), it was again considered that they behaved as ideal gases. The physical exergy of the NCG stream at the reference standard pressure can be determined by Equation 29.

$$e_{ph,NCG} = \sum_i x_{gas,i} \cdot \left[Cp_{gas,i} \cdot (T - T_0) - T_0 \cdot Cp_{gas,i} \cdot \ln \frac{T}{T_0} \right] \quad \text{Equation 29}$$

Table 2 summarizes all the data needed for the calculation of both energy and exergy balances, distinguishing between the experimental and the bibliographic data used in the present work.

Table 2. Experimental and bibliographic data for the calculation of both energy and exergy balances.

Type of material	Experimental data	Bibliographic data
Solid	Mass yield Moisture content Higher heating value Ultimate analysis Specific heat capacity	
Liquid phases	Mass yield Water content Higher heating value Ultimate analysis Composition of the organic fraction	Boiling point of water and the representative organic compound Chemical exergy of water and the representative organic compound Enthalpy at T_0 and T_p of water and the representative organic compound Specific heat capacity of water and the representative organic compound Entropy at T_0 and T_p of water and the representative organic compound
NCG	Mass yield Composition	Chemical exergy of each component Enthalpy of formation of each component Enthalpy at T_0 and T_p of each component Specific heat capacity of each component Entropy at T_0 and T_p of each component

3. Results

3.1. Torrefaction

The results obtained for the energy and exergy balances of torrefaction of SS under different experimental conditions (scenarios shown in Figure 1) are listed in Table 3.

Table 3. $Q_{process}$ and Ψ for torrefaction.

	Products at T_0	Products at T_p	
Torrefaction conditions[a]	$Q_{process}$ (MJ·kg^{-1})	$Q_{process}$ (MJ·kg^{-1})	Ψ (%)
250/13	-0.16	0.45	87.8
250/24	-0.49	0.22	84.9
250/35	-0.14	0.56	82.3
275/13	-0.31	0.39	85.0
275/24[b]	-0.39 ± 0.08	0.37 ± 0.09	85.0 ± 0.7
275/35	-0.45	0.32	85.6
300/13	-0.28	0.50	85.0
300/24	-0.75	0.08	86.2
300/35	-0.74	0.14	86.3

[a]Expressed as Temperature (°C)/time (min). [b]Performed in triplicate.

When SS and the different products were considered to be at the standard reference state (Figure 1.a) the process analyzed was found to be exothermic and to vary between -0.75 MJ·kg$_{SS}^{-1}$ and -0.14 MJ·kg$_{SS}^{-1}$. The process was more exothermic under the most severe torrefaction conditions. As the full recovery of the energy contained in the torrefaction products is not practically feasible, the $Q_{process}$ and the ψ were calculated when the different products were considered to be at torrefaction temperature (Figure 1.b). The process was found to be endothermic at each one of the torrefaction conditions and to vary between 0.08-0.56 MJ·kg$_{SS}^{-1}$. This fact suggested that efficient heat integration within the process could significantly impact the overall thermal behavior of the process. A decrease in the heat required for torrefaction was observed under the most severe torrefaction conditions, as was the case in the study performed by Bates and Ghoniem [51]. The heat required for torrefaction amounted to 6.5% of the total heat required for both drying and torrefaction. The e_{loss} varied between 1.8-2.6 MJ·kg$_{SS}^{-1}$ and the exergy efficiency between 82.3-87.8%.

The results obtained in the present work agree with those obtained by different authors for other types of biomass. Ohliger et al. [52] have estimated that the heat consumption for torrefaction (270-300 °C for 15-60 min) of beechwood chips varied between 0.25-0.99 MJ·kg^{-1}. Granados et al. [37] evaluated the energy and exergy balances of torrefaction (250 °C for 30 min) of different types of residual biomass and found that the heat required for the process varied from endothermic to exothermic, depending on the type of biomass fed. These authors obtained values of exergy efficiency between 60-90% at the process

conditions. Bates and Ghoniem [51] claimed that torrefaction of biomass becomes less endothermic with the increasing severity of torrefaction. According to these authors, torrefaction can be divided into two steps. The first step is exothermic while the exothermicity of the second one depends on the final temperature and the correlations used. Thus, the endothermicity or exothermicity of the process also depends on the final temperature and the correlations used to predict the calorific values, which directly affect the estimation of the enthalpies of formation [51].

3.2. Pyrolysis

The results obtained for the energy and exergy balances of pyrolysis of SS and TSS are shown in Table 4.

Table 4. $Q_{process}$ and Ψ for pyrolysis.

		Pyrolysis feedstock					
		SS		TSS250		TSS275[a]	
		$Q_{process}$ ($MJ \cdot kg^{-1}$)	Ψ (%)	$Q_{process}$ ($MJ \cdot kg^{-1}$)	Ψ (%)	$Q_{process}$ ($MJ \cdot kg^{-1}$)	Ψ (%)
Pyrolysis	Products at T_0	-1.1	-	-0.4	-	-0.2 ± 0.1	-
	Products at T_p	0.1	72	0.5	81	0.5 ± 0.2	83 ± 2
Torrefaction + pyrolysis	Products at T_0	-	-	-0.5	-	-0.5 ± 0.1	-
	Products at T_p	-	-	0.7	71.6	0.6 ± 0.1	73.6 ± 0.9

[a]Performed in duplicate.

First of all, pyrolysis as a standalone process was considered. As shown in Table 4, when the different products were considered to be at the standard reference state (Figure 2.a), the pyrolysis step became more endothermic when SS was first torrefied. When the products were considered to leave the system at the pyrolysis temperature (Figure 2.b) the process turned from exothermic to endothermic, as shown in Table 4. Again, the process was more endothermic when TSS was pyrolyzed. The values of $Q_{process}$ obtained were of the same order of magnitude as those obtained by other authors. Ding and Jiang [28] reported heat for pyrolysis of activated sludge around 1.5 $MJ \cdot kg^{-1}$. Daugaard and Brown [1] reported values of heat for pyrolysis (500 °C) of different types of biomass also around 1.5 $MJ \cdot kg^{-1}$, and claimed that pyrolysis could be considered thermo-neutral since this endothermic value is small. Ansah et al. [9] determined the heat for pyrolysis at 500 °C (including the heat for drying and heating the feedstock and the heat of the reactions) of different components of municipal solid wastes (wood, paper, textiles and polyethylene terephthalate) by DSC analysis, obtaining values between 0.7-2.5 $MJ \cdot kg^{-1}$. These authors reported that the heat for pyrolysis increased with the increase in the torrefaction severity [9].

Doddapaneni et al. [53] observed similar decomposition patterns during pyrolysis, in terms of heat flow (determined by DSC), for Eucalyptus clone. This material torrefied at 250 °C, with an exothermic peak in the range of temperatures between 310-370 °C. However, Eucalyptus clone torrefied at 300 °C did not show this peak, which meant that almost all the hemicellulose present in the raw material had been degraded during torrefaction. Both Eucalyptus clone and torrefied Eucalyptus clone (at 250 and 300 °C) showed an endothermic peak at temperatures between 400-500 °C. These authors reported higher heat flows for pyrolysis of the torrefied material and attributed it to the higher yield of char and the structural changes in biomass during torrefaction.

The exergy efficiency of pyrolysis of SS and TSS varied between 72% and 83 ± 2% (see Table 4) while the e_{loss} varied between 2.4 ± 0.3 $MJ \cdot kg_{TSS}^{-1}$ and 4.1 $MJ \cdot kg_{SS}^{-1}$. Torrefaction of SS was more efficient than pyrolysis of SS from an exergetic point of view. Pyrolysis of TSS showed higher exergy efficiency than pyrolysis of SS. Boateng et al. [12] measured exergy efficiencies between 52.3-66.5% for pyrolysis of different types of biomass, although the model they developed predicted values between 61.0-93.8%. Peters et al. [34] obtained an exergy efficiency around 70% for pyrolysis of hybrid poplar wood at 520 °C, using part of the pyrolysis products as fuels within the process.

When considering the two-step process (torrefaction and pyrolysis) globally, and that the SS and the different products from both torrefaction and pyrolysis were at the standard reference state (Figure 3.a) the $Q_{process}$ was found to be exothermic (-0.5 ± 0.1 $MJ \cdot kg_{SS}^{-1}$), but less exothermic than pyrolysis of SS. When sensible heat from torrefaction and pyrolysis products was recovered, and both steps were considered globally (Figure 3.b), the $Q_{process}$ was found to be around 0.7 $MJ \cdot kg_{SS}^{-1}$ (see Table 4). The two-step process was more endothermic than direct pyrolysis of SS. In any case, the heat needed for the global process was much lower than that needed for drying the material from a moisture content of 77% to a moisture content of 6.5%. The heat required for the two step-process amounted to less than 7% of the total heat required for drying, torrefaction and pyrolysis. The exergy efficiency was between 71.6% and 73.6 ± 0.9% (e_{loss} between 3.9 ± 0.2 $MJ \cdot kg_{TSS}^{-1}$ and 4.2 $MJ \cdot kg_{SS}^{-1}$.) and was similar to that obtained for direct pyrolysis of SS (72%).

3.3. Pyrolysis with catalytic post-treatment of the hot pyrolysis vapors

The results obtained for the energy and exergy balances of pyrolysis of SS and TSS with catalytic post-treatment of the hot pyrolysis vapors are shown in Table 5.

Table 5. $Q_{process}$ and Ψ for pyrolysis with catalytic post-treatment of hot vapors.

		Pyrolysis feedstock					
		SS		TSS250		TSS275[a]	
		$Q_{process}$ ($MJ \cdot kg^{-1}$)	Ψ (%)	$Q_{process}$ ($MJ \cdot kg^{-1}$)	Ψ (%)	$Q_{process}$ ($MJ \cdot kg^{-1}$)	Ψ (%)
Pyrolysis + catalytic step	Products at T_0	-0.2	-	-0.6	-	-0.2 ± 0.3	-
	Products at T_p	0.8	71.3	0.2	71.3	0.6 ± 0.3	73.3± 0.1
Torrefaction + pyrolysis + catalytic step	Products at T_0	-	-	-0.6	-	-0.2 ± 0.2	-
	Products at T_p	-	-	0.4	63.1	0.8 ± 0.2	62.4 ± 0.2

[a]Performed in duplicate.

First of all, the energy and exergy balances considering pyrolysis and catalytic post-treatment of the hot pyrolysis vapors were analyzed (Figure 4.a). When the material (SS or TSS) was fed at the standard reference state and the different products were considered to be also at these conditions, the process was exothermic regardless of whether the SS had been previously torrefied or not. When the products were considered to leave the system at the processes conditions (Figure 4.b), the process was endothermic. The fact that no energy was recovered from the products again turned the process from exothermic to endothermic. Compared to pyrolysis of SS alone, pyrolysis of SS followed by the catalytic post-treatment of the hot vapors was more endothermic. However, the catalytic post-treatment did not have a great effect on the energy requirements of the process when TSS was pyrolyzed. The e_{loss} varied between 4.0 ± 0.1 $MJ \cdot kg^{-1}_{TSS}$ and 4.3 $MJ \cdot kg^{-1}_{SS}$. The exergy efficiency varied between 71.3% and 73.3 ± 0.1% (see Table 5). In the case of TSS, the catalytic post-treatment of the hot pyrolysis vapors significantly decreased the exergy efficiency of the process compared to pyrolysis without this post-treatment.

When torrefaction, pyrolysis and the catalytic post-treatment of the hot pyrolysis vapors were taken into account within the energy and exergy balances (three-step process), and SS and the different products

were considered to be at the standard reference state (Figure 5.a), the $Q_{process}$ was found to be -0.6 $MJ \cdot kg_{SS}^{-1}$ and -0.2 ± 0.2 $MJ \cdot kg_{SS}^{-1}$ when torrefaction was carried out in the auger reactor at 250 °C and 13 min, and at 275 °C and 24 min, respectively. When the three steps were taken into account and the products were considered to leave the system at the processes conditions (Figure 5.b), the $Q_{process}$ was found to be 0.4 $MJ \cdot kg_{SS}^{-1}$ and 0.8 ± 0.2 $MJ \cdot kg_{SS}^{-1}$ when torrefaction was carried out in the auger reactor at 250 °C and 13 min, and at 275 °C and 24 min, respectively. Thus, it seems that the torrefaction did not have an important effect on the energy requirements of the global process. Although the process carried out in three steps was more endothermic than direct pyrolysis of SS, performing the catalytic post-treatment of pyrolysis hot vapors did not impact the energy requirements of the process compared to the two-step process. The heat required for the three-step process amounted to less than 8% of the total heat required including the drying step. The exergy efficiency of the process including the three steps was between 63.1% and 62.4 ± 0.2% (see Table 5), with e_{loss} eround 5.6 $MJ \cdot kg_{SS}^{-1}$. This scenario showed the largest exergy losses, and thus the lowest exergy efficiency, of all the scenarios considered in the present study. Peters et al. [34] calculated an exergy efficiency of around 60% for pyrolysis of hybrid poplar wood at 520 °C and the catalytic hydroupgrading of the bio-oil, using part of the pyrolysis products as fuels within the process. According to these authors, the highest exergy destruction took place during the pyrolysis step.

4. Conclusions

The present paper provides the methodology for calculating the energy and exergy balances for the thermochemical treatment of sewage sludge as well as the results obtained for different scenarios (torrefaction, pyrolysis and pyrolysis with catalytic post-treatment of the hot pyrolysis vapors). The methodology proposed allowed a comparison of the results for the different scenarios. The following conclusions can be drawn from the calculations made:

The results showed that torrefaction endothermicity decreased with torrefaction severity. Pyrolysis of sewage sludge was even less endothermic than torrefaction. The two-step process (torrefaction and pyrolysis) was more endothermic than direct pyrolysis of sewage sludge. However, torrefaction did not show a great effect on the heat requirements when the three steps (torrefaction, pyrolysis and catalytic post-treatment of the hot pyrolysis vapors) were considered globally. The catalytic post-treatment of

pyrolysis hot vapors made the global process more endothermic only in the case of torrefied sewage sludge being pyrolyzed.

The exergy efficiency was higher for standalone pyrolysis of torrefied sewage sludge than for pyrolysis of non-torrefied sewage sludge. However, the exergy efficiency taking into account both torrefaction and pyrolysis was similar to that of direct pyrolysis of sewage sludge. The catalytic post-treatment of the hot pyrolysis vapors decreased the exergy efficiency in the case of torrefied sewage sludge being pyrolyzed. Considering all the steps globally, the three-step process was the least exergy efficient scenario.

For all the scenarios studied, the full energy recovery from the different products turned the processes from endothermic to exothermic. In any case, the heat required for the thermochemical treatment accounted for a small amount of the total heat required for both the drying and the thermochemical treatment of sewage sludge. Therefore, improving the mechanical dehydration of sewage sludge is fundamental to the energy viability of the thermochemical treatment of this waste.

Acknowledgments

This work was supported by the Aragon Government and the European Social Fund (GPT group), and by MINECO and FEDER (project codes CTQ2013-47260-R and CTQ2016-76419-R).

References

[1] Daugaard DE, Brown RC. Enthalpy for pyrolysis for several types of biomass. Energ Fuel 2003;17(4):934-9.

[2] Reed TB, Cowdery CD. Heat flux requirements for fast pyrolysis and a new method for generating biomass vapour. Abs Pap Am Chem S 1987;193:25-CELL.

[3] Lanteigne JR, Laviolette JP, Chaouki J. Determination of enthalpy of pyrolysis from DSC and industrial reactor data: Case of tires. Chem Prod Proc Mod 2015;10(2):97-111.

[4] Mok WSL, Antal MJ. Effects of pressure on biomass pyrolysis. II. Heats of reaction of cellulose pyrolysis. Thermochim Acta. 1983;68(2):165-86.

[5] Chen Q, Yang RM, Zhao B, Li Y, Wang SJ, Wu HW, et al. Investigation of heat of biomass pyrolysis and secondary reactions by simultaneous thermogravimetry and differential scanning calorimetry. Fuel 2014;134:467-76.

[6] Van de Velden M, Baeyens J, Brems A, Janssens B, Dewil R. Fundamentals, kinetics and endothermicity of the biomass pyrolysis reaction. Renew Energy 2010;35(1):232-42.

[7] Manganaro J, Chen B, Adeosun J, Lakhapatri S, Favetta D, Lawal A, et al. Conversion of residual biomass into liquid transportation fuel: An energy analysis. Energ Fuel 2011;25(6):2711-20.

[8] Boukis IP, Grammelis P, Bezergianni S, Bridgwater AV. CFB air-blown flash pyrolysis. Part I: Engineering design and cold model performance. Fuel 2007;86(10-11):1372-86.

[9] Ansah E, Wang LJ, Shahbazi A. Thermogravimetric and calorimetric characteristics during co-pyrolysis of municipal solid waste components. Waste Manage 2016;56:196-206.

[10] Stenseng M, Jensen A, Dam-Johansen K. Investigation of biomass pyrolysis by thermogravimetric analysis and differential scanning calorimetry. J Anal Appl Pyrol 2001;58:765-80.

[11] He F, Yi WM, Bai XY. Investigation on caloric requirement of biomass pyrolysis using TG-DSC analyzer. Energy Conv Manag 2006;47(15-16):2461-9.

[12] Boateng AA, Mullen CA, Osgood-Jacobs L, Carlson P, Macken N. Mass balance, energy, and exergy analysis of bio-oil production by fast pyrolysis. J Energ Resour Asme 2012;134(4).

[13] Hosokai S, Matsuoka K, Kuramoto K, Suzuki Y. Practical estimation of reaction heat during the pyrolysis of cedar wood. Fuel Process Tech 2016;154:156-62.

[14] Capodaglio AG, Callegari A, Dondi D. Microwave-induced pyrolysis for production of sustainable biodiesel from waste sludges. Waste Biomass Valori 2016;7(4):703-9.

[15] Atsonios K, Panopoulos KD, Bridgwater AV, Kakaras E. Biomass fast pyrolysis energy balance of a 1kg/h test rig. Int J Thermod 2015;18(4):267-75.

[16] Yang H, Kudo S, Kuo H-P, Norinaga K, Mori A, Masek O, et al. Estimation of enthalpy of bio-oil vapor and heat required for pyrolysis of biomass. Energ Fuel 2013;27(5):2675-86.

[17] Rosen MA, Dincer I. EXERGY: Energy, environment and sustainable development. 2nd ed. Oxford, Great Britain: Elsevier, 2013.

[18] Cornelissen RL, Hirs GG. The value of the exergetic life cycle assessment besides the LCA. Energy Conv Manag 2002;43(9-12):1417-24.

[19] Rubio Rodríguez MA, Ruyck JD, Díaz PR, Verma VK, Bram S. An LCA based indicator for evaluation of alternative energy routes. Appl Energy 2011;88(3):630-5.

[20] Dewulf J, Van Langenhove H, Muys B, Bruers S, Bakshi BR, Grubb GF, et al. Exergy: Its potential and limitations in environmental science and technology. Environ Sci Technol 2008;42(7):2221-32.

[21] Eboh FC, Ahlstrom P, Richards T. Estimating the specific chemical exergy of municipal solid waste. Energy Sci Eng 2016;4(3):217-31.

[22] Zhang Y, Gao X, Li B, Zhang H, Qi B, Wu Y. An expeditious methodology for estimating the exergy of woody biomass by means of heating values. Fuel 2015;159:712-9.

[23] Song G, Xiao J, Zhao H, Shen L. A unified correlation for estimating specific chemical exergy of solid and liquid fuels. Energy 2012;40(1):164-73.

[24] Bilgen S, Keles S, Kaygusuz K. Calculation of higher and lower heating values and chemical exergy values of liquid products obtained from pyrolysis of hazelnut cupulae. Energy 2012;41(1):380-5.

[25] Gharagheizi F, Mehrpooya M. Prediction of standard chemical exergy by a three descriptors QSPR model. Energy Conv Manag 2007;48(9):2453-60.

[26] Shieh JH, Fan LT. Estimation of energy (enthalpy) and exergy (availability) contents in structurally complicated materials. Energ Source 1982;6(1-2):1-45.

[27] Saidur R, BoroumandJazi G, Mekhilef S, Mohammed HA. A review on exergy analysis of biomass based fuels. Renew Sust Energ Rev 2012;16(2):1217-22.

[28] Ding H-S, Jiang H. Self-heating co-pyrolysis of excessive activated sludge with waste biomass: Energy balance and sludge reduction. Bioresour Technol 2013;133:16-22.

[29] Caballero JA, Front R, Marcilla A, Conesa JA. Characterization of sewage sludges by primary and secondary pyrolysis. J Anal Appl Pyrol 1997;40-1:433-50.

[30] Kim Y, Parker W. A technical and economic evaluation of the pyrolysis of sewage sludge for the production of bio-oil. Bioresour Technol 2008;99(5):1409-16.

[31] Ábrego J, Sánchez JL, Arauzo J, Fonts I, Gíl-Lalaguna N, Atienza-Martínez M. Technical and energetic assessment of a three-stage thermochemical treatment for sewage sludge. Energ Fuel 2013;27(2):1026-34.

[32] Gil-Lalaguna N, Sánchez JL, Murillo MB, Atienza-Martínez M, Gea G. Energetic assessment of air-steam gasification of sewage sludge and of the integration of sewage sludge pyrolysis and air-steam gasification of char. Energy 2014;75:652-62.

[33] Ruiz-Gómez N, Quispe V, Ábrego J, Atienza-Martínez M, Murillo MB, Gea G. Co-pyrolysis of sewage sludge and manure Waste Manage 2017;59:211-21.

[34] Peters JF, Petrakopoulou F, Dufour J. Exergy analysis of synthetic biofuel production via fast pyrolysis and hydroupgrading. Energy 2015;79:325-36.

[35] Keedy J, Prymak E, Macken N, Pourhashem G, Spatari S, Mullen CA, et al. Exergy based assessment of the production and conversion of switchgrass, equine waste, and forest residue to bio-oil using fast pyrolysis. Ind Eng Chem Res 2015;54(1):529-39.

[36] Peters JF, Petrakopoulou F, Dufour J. Exergetic analysis of a fast pyrolysis process for bio-oil production. Fuel Process Tech 2014;119:245-55.

[37] Granados DA, Velasquez HI, Chejne F. Energetic and exergetic evaluation of residual biomass in a torrefaction process. Energy 2014;74:181-9.

[38] Prins MJ, Ptasinski KJ, Janssen FJJG. More efficient biomass gasification via torrefaction. Energy 2006;31(15):3458-70.

[39] Atienza-Martínez M, Fonts I, Lázaro L, Ceamanos J, Gea G. Fast pyrolysis of torrefied sewage sludge in a fluidized bed reactor. Chem Eng J 2015;259:467–80.

[40] Uslu A, Faaij APC, Bergman PCA. Pre-treatment technologies, and their effect on international bioenergy supply chain logistics. Techno-economic evaluation of torrefaction, fast pyrolysis and pelletisation. Energy 2008;33(8):1206-23.

[41] Atienza-Martínez M, Mastral JF, Ábrego J, Ceamanos J, Gea G. Sewage sludge torrefaction in an auger reactor. Energ Fuel 2015;29(1):160-70.

[42] Fonts I, Gea G, Azuara M, Ábrego J, Arauzo J. Sewage sludge pyrolysis for liquid production: A review. Renew Sust Energ Rev 2012;16(5):2781-805.

[43] Atienza-Martínez M, Rubio I, Fonts I, Ceamanos J, Gea G. Effect of torrefaction on the catalytic post-treatment of sewage sludge pyrolysis vapors using γ-Al_2O_3. Chem Eng J 2017;308: 264–74.

[44] Perry RH, Green DW. Perry's Chemical Engineers' Handbook. 7th ed. Australia: McGraw Hill, 1998.

[45] HSC Chemistry 9.0. Outotec.

[46] Szargut J. Exergy method: Technical and ecological applications. Southampton, U.K.: WIT, 2005.

[47] Peduzzi E, Boissonnet G, Marechal F. Biomass modelling: Estimating thermodynamic properties from the elemental composition. Fuel 2016;181:207-17.

[48] Coulson JM, Richardson JF, Sinnott RK. Chemical engineering: An introduction to chemical engineering design. 1st ed. Great Britain: Pergamon, 1983.

[49] Hepbasli A. A key review on exergetic analysis and assessment of renewable energy resources for a sustainable future. Renew Sust Energ Rev 2008;12(3):593-661.

[50] Kaushik SC, Singh OK. Estimation of chemical exergy of solid, liquid and gaseous fuels used in thermal power plants. J Therm Anal Calorim 2014;115(1):903-8.

[51] Bates RB, Ghoniem AF. Biomass torrefaction: Modeling of reaction thermochemistry. Bioresour Technol 2013;134:331-40.

[52] Ohliger A, Förster M, Kneer R. Torrefaction of beechwood: A parametric study including heat of reaction and grindability. Fuel 2013;104:607-13.

[53] Doddapaneni T, Konttinen J, Hukka TI, Moilanen A. Influence of torrefaction pretreatment on the pyrolysis of Eucalyptus clone: A study on kinetics, reaction mechanism and heat flow. Ind Crop Prod 2016;92:244-54.

Table 1. Representative organic compounds chosen for the liquid phases.

Process	Phase	Representative organic compound
Torrefaction	AP_{torr}	Acetic acid
	OP_{torr}	Hexadecanoic acid
Pyrolysis	AP_{pyr}	Acetic acid
	HOP_{pyr}	3-Methylphenol
	LOP_{pyr}	Cholest-4-ene
Pyrolysis with catalytic post-treatment	AP_{cat}	Acetonitrile
	OP_{cat}	3-Methylphenol

Table 2. Experimental and bibliographic data for the calculation of both energy and exergy balances.

Type of material	Experimental data	Bibliographic data
Solid	Mass yield Moisture content Higher heating value Ultimate analysis Specific heat capacity	
Liquid phases	Mass yield Water content Higher heating value Ultimate analysis Composition of the organic fraction	Boiling point of water and the representative organic compound Chemical exergy of water and the representative organic compound Enthalpy at T_0 and T_p of water and the representative organic compound Specific heat capacity of water and the representative organic compound Entropy at T_0 and T_p of water and the representative organic compound
NCG	Mass yield Composition	Chemical exergy of each component Enthalpy of formation of each component Enthalpy at T_0 and T_p of each component Specific heat capacity of each component Entropy at T_0 and T_p of each component

Table 3. $Q_{process}$ and Ψ for torrefaction.

	Products at T_0	Products at T_p	
Torrefaction conditions[a]	$Q_{process}$ (MJ·kg^{-1})	$Q_{process}$ (MJ·kg^{-1})	Ψ (%)
250/13	-0.16	0.45	87.8
250/24	-0.49	0.22	84.9
250/35	-0.14	0.56	82.3
275/13	-0.31	0.39	85.0
275/24[b]	-0.39 ± 0.08	0.37 ± 0.09	85.0 ± 0.7
275/35	-0.45	0.32	85.6
300/13	-0.28	0.50	85.0
300/24	-0.75	0.08	86.2
300/35	-0.74	0.14	86.3

[a]Expressed as Temperature (°C)/time (min). [b]Performed in triplicate.

Table 4. $Q_{process}$ and Ψ for pyrolysis.

		Pyrolysis feedstock					
		SS		TSS250		TSS275[a]	
		$Q_{process}$ (MJ·kg^{-1})	Ψ (%)	$Q_{process}$ (MJ·kg^{-1})	Ψ (%)	$Q_{process}$ (MJ·kg^{-1})	Ψ (%)
Pyrolysis	Products at T_0	-1.1	-	-0.4	-	-0.2 ± 0.1	-
	Products at T_p	0.1	72	0.5	81	0.5 ± 0.2	83 ± 2
Torrefaction + pyrolysis	Products at T_0	-	-	-0.5	-	-0.5 ± 0.1	-
	Products at T_p	-	-	0.7	71.6	0.6 ± 0.1	73.6 ± 0.9

[a]Performed in duplicate.

Table 5. $Q_{process}$ and Ψ for pyrolysis with catalytic post-treatment of hot vapors.

		Pyrolysis feedstock					
		SS		TSS250		TSS275[a]	
		$Q_{process}$ ($MJ \cdot kg^{-1}$)	Ψ (%)	$Q_{process}$ ($MJ \cdot kg^{-1}$)	Ψ (%)	$Q_{process}$ ($MJ \cdot kg^{-1}$)	Ψ (%)
Pyrolysis + catalytic step	Products at T_0	-0.2	-	-0.6	-	-0.2 ± 0.3	-
	Products at T_p	0.8	71.3	0.2	71.3	0.6 ± 0.3	73.3± 0.1
Torrefaction + pyrolysis + catalytic step	Products at T_0	-	-	-0.6	-	-0.2 ± 0.2	-
	Products at T_p	-	-	0.4	63.1	0.8 ± 0.2	62.4 ± 0.2

[a]Performed in duplicate.

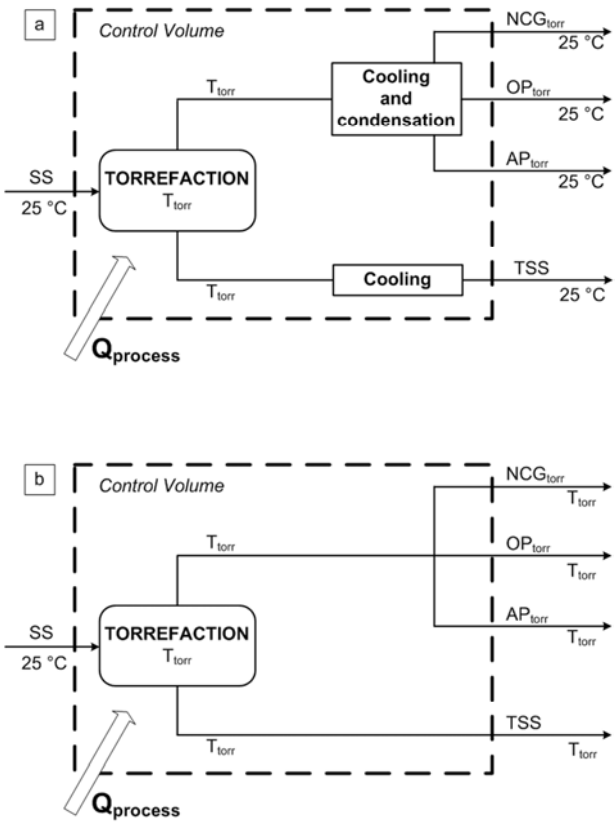

Figure 1. Control volume for torrefaction. (a) Products at the standard reference state. (b) Products at process conditions.

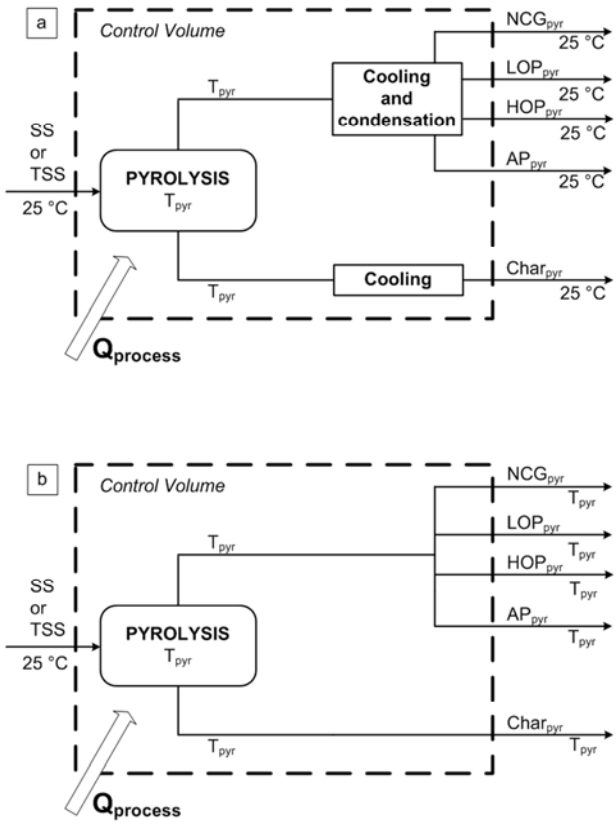

Figure 2. Control volume for pyrolysis. (a) Products at the standard reference state. (b) Products at process conditions.

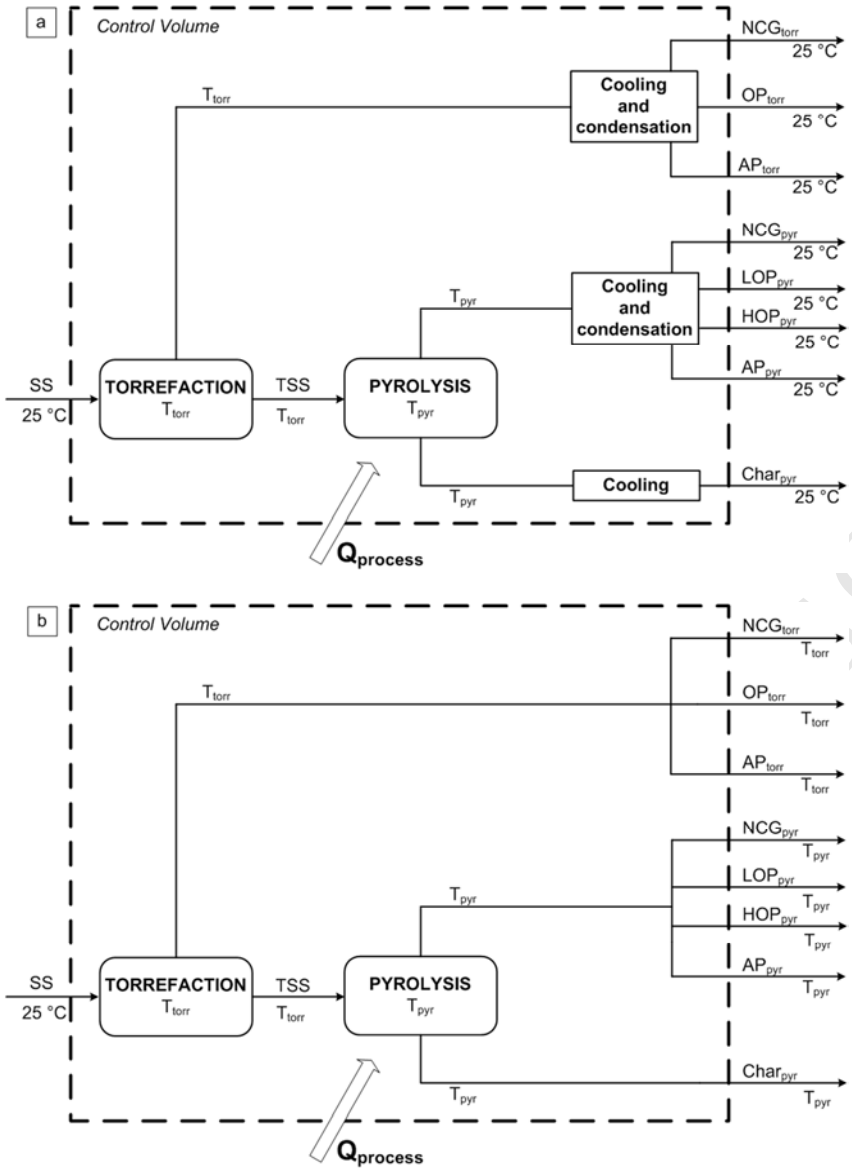

Figure 3. Control volume for pyrolysis including the torrefaction step. (a) Products at the standard reference state. (b) Products at process conditions.

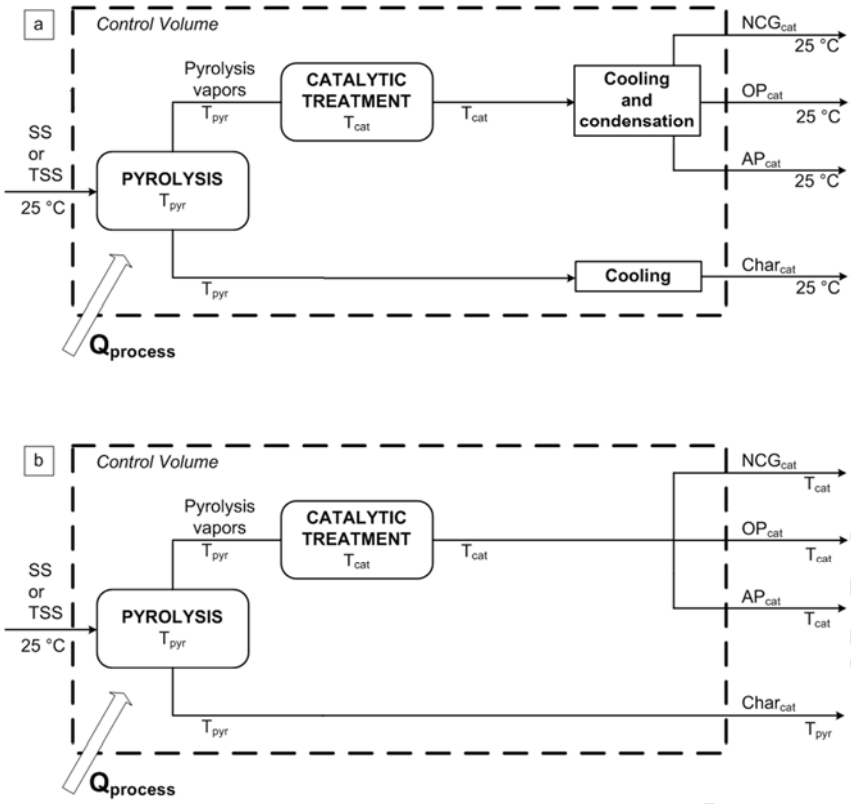

Figure 4. Control volume for pyrolysis with catalytic treatment of the vapors. (a) Products at the standard reference state. (b) Products at process conditions.

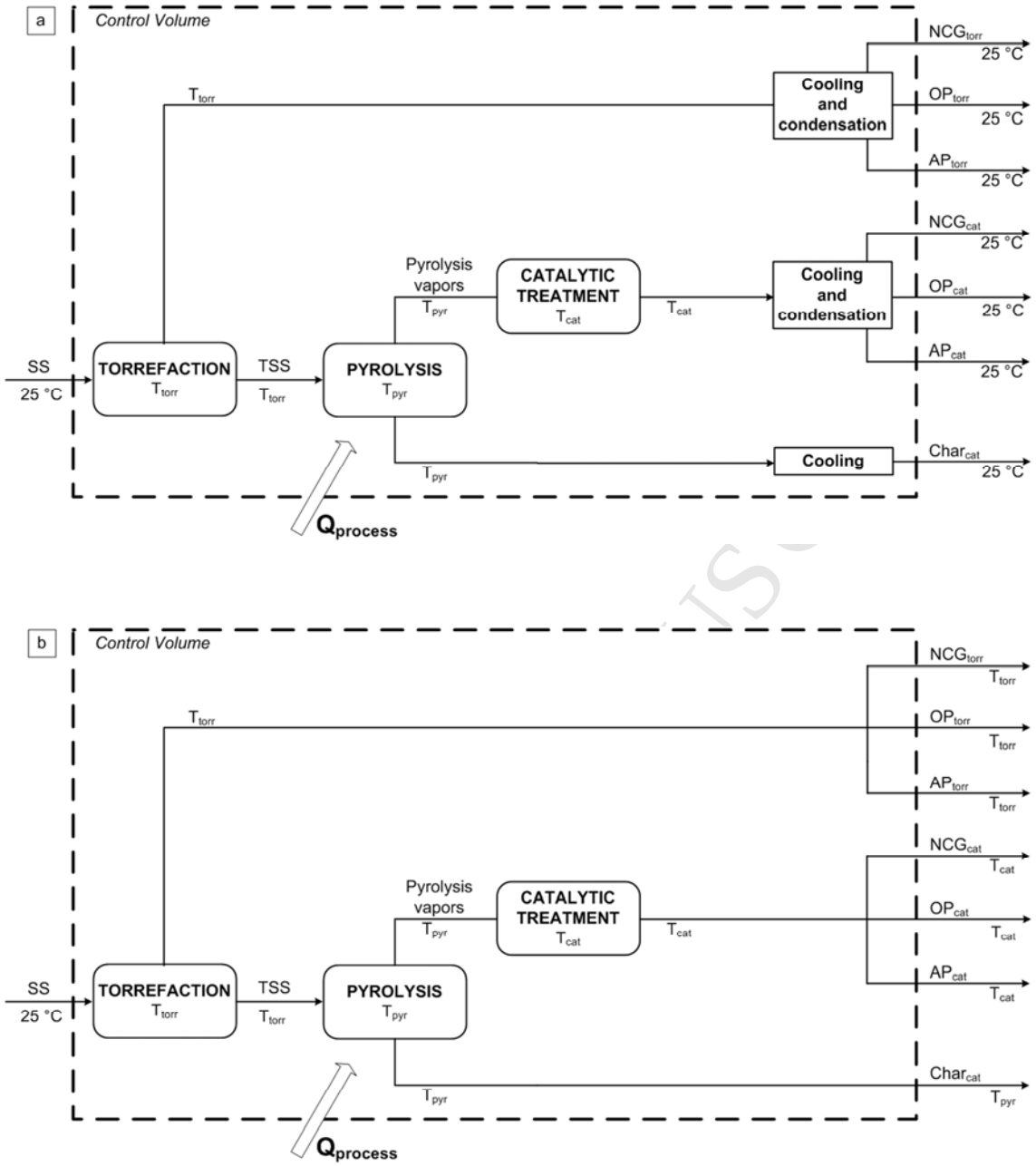

Figure 5. Control volume for pyrolysis with catalytic post-treatment of the hot vapors, including the torrefaction step. (a) Products at the standard reference state. (b) Products at process conditions.

HIGHLIGHTS

- Energy/exergy analyses for thermochemical treatment of sewage sludge were assessed.
- A detailed calculation methodology was provided.
- The energy recovery from the products favored the exothermicity.
- The three-step pyrolysis process was the least exergy-efficient scenario.